

International Journal of Modern Physics E
 © World Scientific Publishing Company

Low-lying states in ^{30}Mg : a beyond relativistic mean-field investigation

J. M. Yao, Z. X. Li, J. Xiang, H. Mei

*School of Physical Science and Technology,
 Southwest University, Chongqing 400715 China*

J. Meng*

*State Key Laboratory of Nuclear Physics and Technology,
 School of Physics, Peking University, Beijing 100871, China
 School of Physics and Nuclear Energy Engineering,
 Beihang University, Beijing 100191, China*

The recently developed model of three-dimensional angular momentum projection plus generator coordinate method on top of triaxial relativistic mean-field states has been applied to study the low-lying states of ^{30}Mg . The effects of triaxiality on the low-energy spectra and E0 and E2 transitions are examined.

1. Introduction

Radioactive nuclear beam facilities and gamma ray detectors have in recent years allowed one to study spectroscopy of the low-lying excited states for exotic nuclei. It provides rich information about the nuclear structure, including evolution of shell structure and collectivity, nuclear shape and quantum phase transition^{1,2}, decoupling of neutrons and protons³. Presently, much interest is focused on the measurement of the energies of the first 2^+ , or 4^+ states and of the reduced transition probabilities ($B(E2)$ -values) from the first 2^+ to the ground state (0_1^+). These are fundamental quantities which can be used to disclose the nuclear shapes and shell structure. A high energy of the first excited 2^+ state and a corresponding low $B(E2; 0_1^+ \rightarrow 2_1^+)$ electromagnetic transition strength, are characteristic signatures of shell closures and vice versa. In Figure 1, we plot the two-neutron separation energy as a function of proton number for different isotones. Large gaps are found between two neighbor isotones with neutron number around $N = 8, 20, 28, 50$, etc. In addition, one notices that the gaps, for instance with $N = 20$ and 28 , are decreasing when one goes to neutron-rich regions. The evolution information of shell structure is reflected in nuclear low-lying states, for example, the first 2^+ excitation energy as shown in the lower part of Figure 1. It is seen clearly that the $E_x(2_1^+)$ s in ^{32}Mg and ^{30}Ne are much lower than those in other $N = 20$ isotones, indicating

*mengj@pku.edu.cn

2 *J. M. Yao et al.,*

the erosion of magic number $N = 20$. Similar situation has been shown in $N = 28$ isotones as well. Therefore, the study of low-lying states provides us an important way to examine the shell structure in exotic nuclei and becomes one of the major research fields of the nuclear structure community.

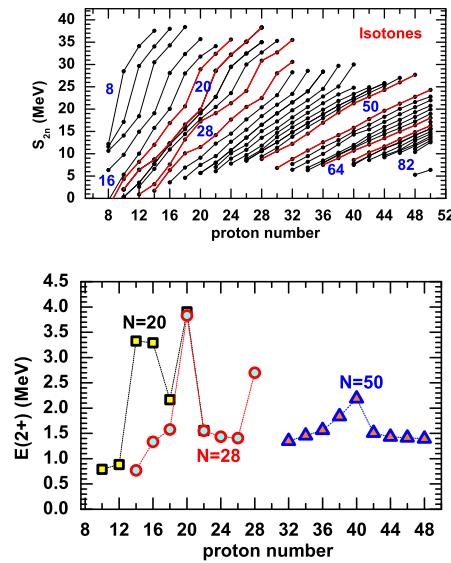


Fig. 1. (Upper panel) Two-neutron separation energy S_{2n} as a function of proton number for different isotones. (Lower panel) Systematic variation of the first excited 2^+ state $E_x(2^+)$ in isotones with $N = 20, 28$ and 50 . All experimental data are taken from Ref.[4].

An alternative approach to the large scale shell model calculations for nuclear low-lying states is the new beyond mean field theories⁵. In recent years several accurate and efficient models and algorithms have been developed that perform the restoration of symmetries broken by the static nuclear mean field and take into account fluctuations around the mean-field minimum. The most effective approach to configuration mixing calculations is the generator coordinate method (GCM). With the simplifying assumption of axial symmetry, GCM configuration mixing of one-dimensional angular-momentum projected (1DAMP) and even particle-number projected (PNP) quadrupole-deformed mean-field states, has become a standard tool in nuclear structure studies with Skyrme energy density functionals⁶, the density-dependent Gogny force⁷, and relativistic density functionals⁸. A variety of structure phenomena has been analyzed using this approach, such as, the structure of low-spin deformed and superdeformed collective states^{9,10,11}, shape coexistence in Kr and Pb isotopes^{12,13}, shell closures in the neutron-rich Ca, Ti and Cr isotopes¹⁴ and shape transition in Nd isotopes^{15,16}.

Recently, the 1DAMP+GCM framework has been extended to include triax-

ial shapes, which makes it possible to study the nuclear low-lying states with the consideration of effects from restoration of rotation symmetry in full Euler space and shape fluctuation in β - γ plane. Along this direction, the 3DAMP+GCM models with PNP have been developed, based on the self-consistent Hartree-Fock-Bogoliubov approach with Skyrme forces¹⁷ and the Gogny force¹⁸. In these models, seven degrees of freedom (three Euler angles + two deformation parameters + two gauge angles for protons and neutrons) should be considered, which makes the calculations very time-consuming. Therefore, only illustrative calculations have been done with these models. In the mean time, the 3DAMP+GCM model on top of the relativistic mean-field has also been developed^{19,20,21}. In the relativistic 3DAMP+GCM model, the prescription given in Refs.^{22,23} has been used to restore approximately the correct mean values of the nucleon numbers by adding constraint terms for nucleon numbers to the transition energy functional.

In this report, the recently developed relativistic 3DAMP+GCM model will be outlined and its applications to the low-lying states of ^{30}Mg will be presented. The effects of triaxiality on the low-energy spectra and transitions will be examined.

2. The relativistic 3DAMP+GCM model

In the relativistic 3DAMP+GCM model, we first perform the triaxial relativistic point-coupling model plus BCS calculations with quadratic constraints on the mass quadrupole moments by minimizing the following energy functional

$$E'[\rho_i, j_i^\mu] = E[\rho_i, j_i^\mu] + \sum_{\mu=0,2} \frac{C_\mu}{2} (\langle \hat{Q}_{2\mu} \rangle - q_{2\mu})^2, \quad (1)$$

that is a functional of four types (S, V, TS, TV) of densities and currents. $\langle \hat{Q}_{2\mu} \rangle$ denotes the expectation value of the mass quadrupole operator, $q_{2\mu}$ is the triaxial deformation parameter, and C_μ is the stiffness constant. This procedure generates a large set of highly correlated intrinsic deformed states $|\Phi(q)\rangle$. There are successful non-linear versions, PC-F1²⁴, PC-PK1²⁵ and density-dependent version, DD-PC1²⁶ of relativistic energy functionals that can be used in Eq.(1). The pairing correlations, for open-shell nuclei, are taken into account by augmenting the following pairing energy functional,

$$E[\kappa] = - \sum_{\tau} \int d\mathbf{r} \frac{V_{\tau}}{4} \kappa_{\tau}^*(\mathbf{r}) \kappa_{\tau}(\mathbf{r}) \quad (2)$$

with separately adjustable pairing strengths $V_{p/n}$ for protons and neutrons. The anomalous density (pairing tensor) $\kappa_{\tau}(\mathbf{r})$ is determined by the occupation probability coefficient v_k and density $\rho_k(\mathbf{r})$ of single-particle state,

$$\kappa(\mathbf{r}) = -2 \sum_{k>0} f_k u_k v_k \rho_k(\mathbf{r}), \quad (3)$$

where f_k is an energy-dependent smooth cutoff factor used to simulate the effects of finite-range. Alternatively, one can use a separable pairing force²⁷ in the pairing

4 *J. M. Yao et al.*,

channel. The results of low-lying states with the separable pairing force will be given elsewhere.

The nuclear wave function $|\Psi_\alpha^{JM}\rangle$ with good angular momentum and shape fluctuation is obtained by projecting the intrinsic states $|\Phi(\beta, \gamma)\rangle$ onto good angular momentum (K-mixing) and performing GCM calculations (configuration mixing),

$$|\Psi_\alpha^{JM}\rangle = \int d\beta d\gamma \sum_{K \geq 0} f_\alpha^{JK}(\beta, \gamma) \frac{1}{(1 + \delta_{K0})} [\hat{P}_{MK}^J + (-1)^J \hat{P}_{M-K}^J] |\Phi(\beta, \gamma)\rangle \quad (4)$$

The weight functions f_α^{JK} are determined from the solution of Hill-Wheeler-Griffin (HWG) integral equation

$$\int dq' \sum_{K' \geq 0} [\mathcal{H}_{KK'}^J(q, q') - E_\alpha^J \mathcal{N}_{KK'}^J(q, q')] f_\alpha^{JK'}(q') = 0, \quad (5)$$

where \mathcal{H} and \mathcal{N} are the angular-momentum projected GCM kernel matrices of the Hamiltonian and the Norm, respectively. q is the abbreviation of triaxial deformation parameters (β, γ) .

The electromagnetic moments and transition strengths of low-lying states are evaluated with the nuclear wave function $|\Psi_\alpha^{JM}\rangle$. More details about the relativistic 3DAMP+GCM model can be found in Refs. 20,21.

3. Low-lying states in ^{30}Mg

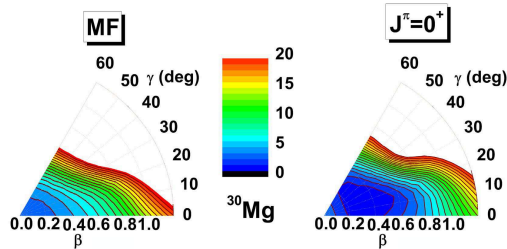


Fig. 2. Self-consistent RMF+BCS triaxial quadrupole energy surface and angular-momentum-projected energy surface with $J^\pi = 0^+$ from the 3DAMP+GCM calculations with the effective interaction PC-F1. All energies are normalized with respect to the binding energy of the absolute minimum. The contours join points on the surface with the same energy. The difference between neighboring contours is 1.0 MeV.

Figure 2 shows the self-consistent RMF+BCS triaxial quadrupole energy surface and angular-momentum-projected energy surface with $J^\pi = 0^+$ from the 3DAMP+GCM calculations with the effective interaction PC-F1. It is seen that there is an evident near-spherical minimum in mean-field energy surface of ^{30}Mg .

However, this minimum shifts to a relative large deformed shape with $\beta = 0.4$ and $\gamma = 20^\circ$. The dynamic correlation energy from the restoration of rotational symmetry is about 2.7 MeV. The projected energy surface becomes soft in both β and γ directions around the minimum, indicating the existence of large shape fluctuations. This phenomenon can be seen from the probability distribution of ground state in Fig. 3.

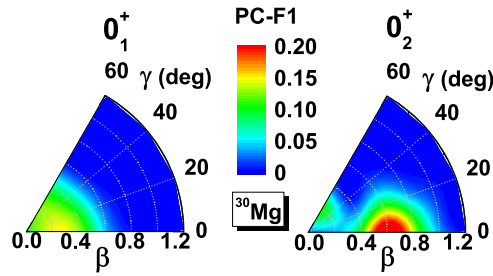


Fig. 3. Contour plots of the probability distribution of collective wave functions for the lowest two 0^+ states.

To examine the effects of triaxiality on the low-energy spectra and transitions, we present the spectroscopic results from both 1D- (frozen $\gamma = 0^\circ, 180^\circ$) and 3D-AMP+GCM calculations in Table 1, where the results of 1DAMP+GCM calculations with the non-relativistic Gogny force and corresponding experimental data²⁸ are given for comparison. It shows that the inclusion of triaxiality in the 3DAMP+GCM calculations with the PC-F1 brings the results of $E_x(2_1^+)$, $E_x(0_2^+)$ and $E0$ transition strength $\rho_{21}^2(E0) \times 10^3$ more closer to the data.

Table 1. Results from both 1D and 3DAMP+GCM calculations with the PC-F1 force. Both the non-relativistic calculation results with Gogny force and experimental data are taken from Ref.[28].

	$E_x(2_1^+)$ (MeV)	$E_x(0_2^+)$ (MeV)	$\rho_{21}^2(E0) \times 10^3$	$B(E2; 0_1^+ \rightarrow 2_1^+)$ ($e^2\text{fm}^4$)	$B(E2; 0_2^+ \rightarrow 2_1^+)$ ($e^2\text{fm}^4$)
Exp.	1.482	1.789	26.2 ± 7.5	241(31)	53(6)
3D(PC-F1)	1.721	2.864	24.72	277	68
1D(PC-F1)	1.882	3.275	15.56	257	47
1D(Gogny-D1S)	2.03	2.11	46	334.6	181.5

4. Summary

In conclusion, the recently developed relativistic 3DAMP+GCM model has been outlined and its applications to the low-lying states of ^{30}Mg has been presented. It

6 *J. M. Yao et al.,*

has been found that ^{30}Mg has large shape fluctuations in both β and γ directions around the triaxially deformed minimum. The effects of triaxiality on the low-energy spectra and transitions have been shown to be important to reproduce the corresponding experimental data.

Acknowledgements

J.M.Y would like to express his deep gratitude to all his collaborators, in particular to K. Hagino, Z. P. Li, D. Pena Arteaga, P. Ring, and D. Vretenar for the active collaboration over many years on the topics addressed in this paper. This work has been supported in part by the Major State 973 Program 2007CB815000 and the National Natural Science Foundation of China under Grant Nos. 10947013, 10975008, 10705004 and 10775004, the Southwest University Initial Research Foundation Grant to Doctor (No. SWU109011).

References

1. R. F. Casten, *Nature Physics*, 2 (2006) 811.
2. P. Cejnar, *Rev. Mod. Phys.* 82 (2010) 2155.
3. N. Imai et al., *Phys. Rev. Lett.* 92 (2004) 062501.
4. National Nuclear Data Center, BNL (<http://www.nndc.bnl.gov/>).
5. M. Bender et al., *Rev. Mod. Phys.* 75 (2003) 121.
6. A. Valor, P. H. Heenen, and P. Bonche, *Nucl. Phys. A* 671, 145 (2000).
7. R. Rodriguez-Guzman, J. L. Egido, and L. M. Robledo, *Nucl. Phys. A* 709, 201 (2002).
8. T. Nikšić, D. Vretenar, and P. Ring, *Phys. Rev. C* 73, 034308 (2006).
9. R. R. Rodriguez-Guzman et al., *Phys. Rev. C* 62 (2000) 054308 .
10. M. Bender, H. Flocard, and P. H. Heenen, *Phys. Rev. C* 68 (2003) 044321 .
11. M. Bender et al., *Phys. Rev. C* 69 (2004) 064303.
12. R. R. Rodriguez-Guzman et al., *Phys. Rev. C* 69 (2004) 054319.
13. M. Bender, P. Bonche, and P.-H. Heenen, *Phys. Rev. C* 74 (2006) 024312.
14. T. R. Rodriguez and J. L. Egido, *Phys. Rev. Lett.* 99 (2007) 062501.
15. T. Nikšić et al., *Phys. Rev. Lett.* 99 (2007) 092502.
16. T. R. Rodriguez and J. L. Egido, *Phys. Lett. B* 663 (2008) 49.
17. M. Bender and P.-H. Heenen, *Phys. Rev. C* 78, 024309 (2008).
18. T. R. Rodriguez and J. L. Egido, *Phys. Rev. C* 81, 064323 (2010)
19. J. M. Yao, J. Meng, D. P. Arteaga, and P. Ring, *Chin. Phys. Lett.* 25 (2008) 3609.
20. J. M. Yao, J. Meng, P. Ring, D. Pena Arteaga, *Phys. Rev. C* 79 (2009) 044312.
21. J. M. Yao, J. Meng, P. Ring, D. Vretenar, *Phys. Rev. C* 81 (2010) 044311.
22. K. Hara, A. Hayashi, and P. Ring, *Nucl. Phys. A* 385, 14 (1982).
23. P. Bonche et al., *Nucl. Phys. A* 510, 466 (1990).
24. T. Burvenich *et al Phys. Rev. C* 65 (2002) 044308.
25. P. W. Zhao, Z. P. Li, J. M. Yao, and J. Meng, arXiv:1002.1789v1 [nucl-th].
26. T. Nikšić, D. Vretenar, and P. Ring, *Phys. Rev. C* 78 (2008) 034318.
27. Y. Tian, Z. Y. Ma, P. Ring, *Phys. Lett. B* 676 (2009) 44.
28. W. Schwerdtfeger *et al., Phys. Rev. Lett.* 103 (2009) 012501.